Urol Res (2011) 39:29–37
DOI 10.1007/s00240-010-0280-7

ORIGINAL PAPER

Effect of uropathogens on in vitro encrustation of polyurethane double J ureteral stents

Nandakumar Venkatesan · Sunil Shroff · Karthik Jeyachandran · Mukesh Doble

Received: 5 June 2009 / Accepted: 15 May 2010 / Published online: 2 June 2010

Abstract Polyurethane stents are used when there is an obstruction to the flow of urine. A majority of the patients with such stents are at the risk of urinary tract infection and salt encrustation. The present study is aimed at analyzing the in vitro encrustation of calcium oxalate and other salts in the presence of common uropathogens (*E. coli* and *P. mirabilis*) on films made from Tecoflex®, a commercial grade polyurethane. In the absence of uropathogens, sodium ions and ammonia favor calcium adsorption whereas magnesium ions greatly depress it, resulting in increased hydrophillicity of the stent. With *E. coli*, Mg ions enhance the encrustation of calcium, whereas the other salts decrease its deposition. In case of *P. mirabilis*, irrespective of the type of salt, it enhances calcium encrustation except in the presence of sodium ions. Adhesion of uropathogens to the stent surface was higher in the presence of bovine serum albumin. Understanding the dynamics between various salts and microorganism in the urine, and urine–stent interface would aid in designing stents that are inert, resist encrustation and biofilm formation.

Keywords Polyurethane · Encrustation · Bacterial adhesion · Metal ions · Albumin

N. Venkatesan · M. Doble (✉)
Department of Biotechnology,
Indian Institute of Technology Madras, Chennai, India
e-mail: mukeshd@iitm.ac.in; mukesh.doble0@gmail.com

S. Shroff · K. Jeyachandran
Department of Urology, Sri Ramachandra University
and Research Institute, Chennai, India

Introduction

Ureteral stent is a narrow hollow plastic tube that runs inside the ureter between the kidney and the bladder. It aids the flow of urine and is profoundly used in the treatment of patients with urological disorders including obstructive uropathy, ureteric injury, primary or malignant carcinomas, and radiation or retroperitoneal fibrosis [1]. Long term ureteral stenting is hindered by encrustation, biofilm formation, and stent fracture. Encrustation or formation of crust develops due to the rapid precipitation of urinary salts with the increasing alkalinity, and this is attributed to the effect of urease-producing organism, *Proteus mirabilis*, resulting in the blockage of stent lumen. Bacterial colonization begins with the deposition of protein on the biomaterial surface, ureteral stent does not induce proteinuria; but adsorption of the host protein to the surface of polymer is an immediate event after stenting, resulting in conditioning film formation which provides multiple binding sites for bacterial adhesion, and in turn this binding proceeds from an reversible attachment to irreversible adhesion leading to biofilm formation which contains proteins, glycoprotein, electrolytes, and others synthesized by the bacteria [2]. Biofilm is the consequence of adherence and multiplication of a single bacterium forming the base film, followed by surface film, eventually causing urinary tract infection (UTI) [3]. The reported rates for bacterial colonization in adults, in less than a week after stenting ranges from 28 to 90%, and the rates for UTI range from 7 to 34% [4]. It is hypothesized that increased risks are due to the formation of an organic layer on the polymer surface, consisting of proteins which can bind ions, aggregate crystals, and support microbial attachment [5, 6]. Bacterial adhesion is attributed to the development of a localized gel-like organic medium which surrounds the bacterial cell; this capsule consists of an

exopolysaccharide glycocalyx polymer which facilitates the adhesion of individual bacterial cells to the stent surface [7]. Many studies have highlighted the presence of an organic matrix in the calculi, formed by urinary proteins which aggregate with lipids and polysaccharides, forming macromolecular templates where salts precipitate [8].

Most widely used biomaterials include silicone, polyurethane, and polyurethane-based polymers [9] and they are not satisfactory owing to the issues stated above. Coating of antimicrobial agents or hydrogels on the polymer surface and use of various polymer blends by modifying the substrate polymer are followed in order to enhance the inert nature of the biomaterial towards encrustation and bacterial colonization [10]. But all these approaches have proved to be less effective clinically. Many studies are carried out on encrustation and bacterial colonization, but there is not enough studies on the kinetics of encrustation under various conditions and the interplay between different salts in the sterile urine and bacterial urine. The present study is aimed at analyzing the in vitro encrustation of calcium oxalate (predominant encrustant on ureteral stents) and other salts on films made from Tecoflex®, commercial grade polyurethane which is used for making ureteral stents. Encrustation in the presence and absence of uropathogens, effect of encrustation, and conditioning film on the polymer surface are also analyzed. *E. coli* and *P. mirabilis* are the common uropathogens involved in this study; the former is a common intestinal pathogen and it colonizes from the bladder to the kidney and is responsible for the ascending urinary tract infection. *P. mirabilis* is of great importance because it is an urease positive organism, which catalyzes the hydrolysis of urea to ammonia and carbon dioxide, thereby increasing the alkalinity of urine and enhancing the precipitation of inorganic salts [11].

Materials and methods

Chemicals

Calcium chloride, Sodium oxalate, Magnesium sulfate hepta-hydrate, Ammonium chloride, Urea, Sodium sulfate, Sodium phosphate, Sodium dihydrogen phosphate, and Sodium citrate were purchased from Merck, India. Bovine Serum Albumin (BSA), Nutrient agar and Nutrient broth were purchased from Himedia, India.

Preparation of polyurethane film

The commercial Tecoflex® polyurethane (PU) stents were dissolved in 5% (w/v) chloroform for 24 h. 30 ml of this solution was transferred to a glass petri-dish and was covered with an inverted funnel and placed in a fume-cupboard at room temperature for a period of 24 h during which the chloroform evaporates, leaving a thin film of PU. The cast film was incised into 1×1 cm dimension and kept immersed in 99% ethanol for 24 h before further use [12].

Preparation of salt solution

Various combinations of salt solutions (urea + sodium hydrogen phosphate; urea + magnesium sulfate heptahydrate; urea + ammonium chloride) used as a media are tabulated in Table 1. 10 ml of 0.909 M calcium chloride solution and 60 ml of 0.05 M sodium oxalate solution were added to all these combinations. The pH of the solution was made 6 by adding either 1 N hydrochloric acid or sodium hydroxide. Artificial urine and salt solutions were sterilized by a method as reported earlier [13].

Preparation of protein solution

Bovine serum albumin fraction-V was considered as a model for HSA since it mimics the human serum albumin with respect to amino acid residues and also shares a functional similarity which is a reflection of their structural similarity, sharing 6 antigenic sites. The immunologic relationship between HSA and BSA is very similar that there was only 15% cross-reaction between them. Moreover, the non-specific protein-binding property of bovine albumin makes it an ideal molecule, as a substitute for HSA to understand the protein—bacterial and protein—polymer interaction in the urinary environment [14]. 10 mg of BSA was dissolved in 100 ml of ultra pure water and was sterilized before further use.

Bacterial strains and media

Gram negative, *E. coli* and *P. mirabilis* strains, for this study, were purchased from NCIM (National Collection of Industrial Microorganisms, Pune, India). The strains from the stock were cultured with nutrient agar and grown with nutrient broth. Bacteria grown overnight were diluted to 1:10 and grown further under similar conditions for 2 h in the artificial urine solution. This incubated culture was plated on nutrient agar plate to determine the initial inoculum dosage [15].

Experimental protocol

1. Encrustation of salts

The kinetics of encrustation of salts on PU film was assessed in McCartney bottles, with few modifications to a previously reported method [16]. Around 5 ml of these test solutions (Table 1) was added to sterile tubes. Three sterilized polyurethane films were then dropped into each tube

Table 1 Composition of various solutions used in the current study

Solution	Combination of salts	Concentration (g L^{-1})
Solution 1	Urea	1.6
Solution 2	Sodium hydrogen phosphate	6.8
	Urea	1.6
Solution 3	Magnesium sulfate hepta hydrate	1.143
	Urea	1.6
Solution 4	Ammonium chloride	4.643
	Urea	1.6
Solution 5	Artificial urine	Equal volume of solution A and B
	Solution A	
	Calcium chloride dehydrate	1.765
	Sodium sulfate	4.862
	Magnesium sulfate hepta hydrate	1.143
	Ammonium chloride	4.643
	Potassium chloride	12.130
	Solution B	
	Sodium hydrogen phosphate-monobasic	6.8
	Sodium hydrogen phosphate	0.869
	Tri sodium citrate dehydrate	1.168
	Sodium chloride	13.545

Calcium chloride = 0.909 M, disodium oxalate = 0.05 M

under sterile condition. These tubes were incubated in an orbital shaker at 200 rpm and 37°C for 5 weeks.

2. Encrustation in the presence of *E. coli* or *P. mirabilis*

500 µl of 2 h incubated culture of gram-negative *E. coli* or *P. mirabilis* was added to the test tubes containing 5 ml of the test solution (prepared as mentioned before). Then these tubes were incubated in shaker at 200 rpm and 37°C for 5 weeks. Experiments were carried out in triplicates. The amount of salt encrusted, pH, and the amount of microbial colonies adhered were analyzed on weekly basis [15].

3. Protein adhesion in the presence of *E. coli* or *P. mirabilis*

Protein solution was prepared and sterilized in six conical flasks which were grouped into three sets. Around five to six sterile PU films were added into each of the flasks under sterile conditions. The first set of flasks served as a control. To the second and third test sets 500 µl of 2 h incubated culture of *E. coli* and *P. mirabilis* were added, respectively. The experiments were carried out in duplicates. The amount of protein adhered was measured by Bradford assay and the number of colony-forming units was measured by spread plate method [16].

Chemical analysis of encrustation

Films were removed on weekly basis and soaked in 5% (vol/vol) of hydrochloric acid, sonicated at low frequency in water to remove the adhered encrustants. The amount of calcium and magnesium encrusted on the films was determined with Inductively Coupled Plasma–Optical Emission Spectrometer (Perkin Elmer-Optima 5300 DV ICP–OES) [17].

Bacterial adhesion assay

After incubation, each film was transferred to a sterile eppendorf tube containing l ml of saline and was sonicated in water for 30 s. After a tenfold serial dilution they were spread on nutrient agar plates. The number of viable bacteria dislodged in saline after sonication was calculated as colony-forming units (CFU). These values represent the maximum number of bacteria that are able to adhere to the film [18, 19], and the average results from multiple readings are reported here.

Contact angle measurements

The surface hydrophobicity and heterogeneity of the films were determined by measuring the contact angle using a Kruss Easy drop goniometer (KRUSS, DSA II GmbH, Germany). A drop of ultra pure water was placed on the polymer film and the angle formed at the solid–liquid interface was measured on each side, and the mean values were determined by averaging the measurements on two independent specimens [20].

AFM imaging

Surface topography was determined with a scanning probe atomic force microscope (NANOSURF EASY SCAN 2 AFM VERSION 2) in contact mode. A rectangular silicon nitride cantilever of 200 µm length and 40 µm width with a force constant of 3 Nm^{-1} was used for the measurement.

FTIR analysis

Films removed on weekly basis were sonicated to remove the adherent particles. FT-IR (Bruker Tensor-27) spectra of the samples were recorded in 400–4,000 cm^{-1} range with an accuracy of 4 cm^{-1} in the transmittance mode.

Results

ICP analysis gives an insight into the amount of cations encrusted in the (1) presence and absence of uropathogens and (2) role of individual salt on its encrustation. Figures 1 and 2 explain the kinetics of encrustation of calcium with calcium oxalate and artificial urine, respectively, in the presence and absence of *E. coli/P. mirabilis*. In the case of artificial urine, the amount encrusted reached equilibrium by the third week, whereas with the organisms, the encrustation prolonged (Fig. 2). In the case of sterile solution 1, encrustation reached equilibrium only by the fifth week. Figure 3 shows the amount of calcium encrusted from each of the five solutions at the end of 5 weeks in the presence and absence of *E. coli/P. mirabilis*. With *E. coli*, calcium encrustation was less in the case of solutions 2 and 4 and with *P. mirabilis* it was less only in solution 2, whereas in case of solutions 3 and 5 both the organisms increased calcium encrustation. Encrustation also included a significant amount of magnesium and phosphorous on the polymer surface. Figures 4 and 5 show the surface density of magnesium and phosphorous at the end of fifth week. *P. mirabilis* also favors the encrustation of magnesium (Fig. 4). The contact angle of virgin polymer was 87.6° and after analysis there was a significant decrease in all the cases (surface became more hydrophilic). The surface of the film became more hydrophilic upon encrustation in the absence of organisms than in their presence (Fig. 6). Protein deposition was higher with *P. mirabilis* than with *E. coli* (Fig. 7). Total protein reported here includes bovine serum albumin as well as the extra cellular protein secreted by the microorganisms, which was higher with *P. mirabilis*. Adsorption of bovine serum albumin alone makes the surface hydrophilic but with an increase in time it turns the surface hydrophobic whereas *E. coli* turns the surface more hydrophilic than *P. mirabilis* (Fig. 8).

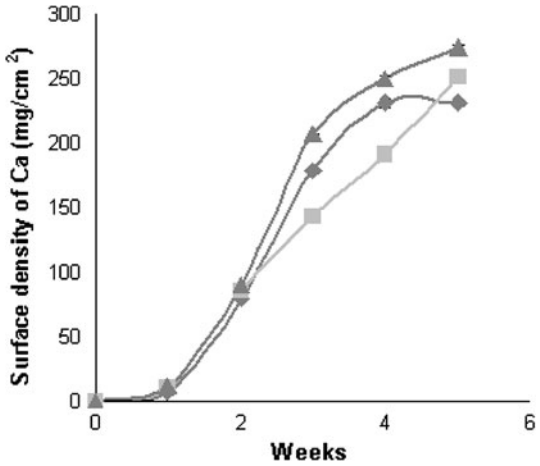

Fig. 1 Kinetics of encrustation of calcium with solution 1 in the presence of *E. coli* and *P. mirabilis*. *Filled diamonds* without microorganisms, *grey squares* with *E. coli*, *filled triangles* with *P. mirabilis*

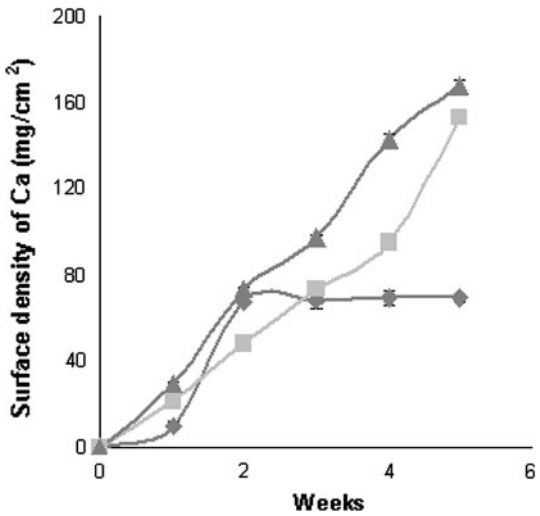

Fig. 2 Kinetics of encrustation of calcium with solution 5 in the presence of *E. coli* and *P. mirabilis*. *Filled diamonds* without microorganisms, *grey squares* with *E. coli*, *filled triangles* with *P. mirabilis*

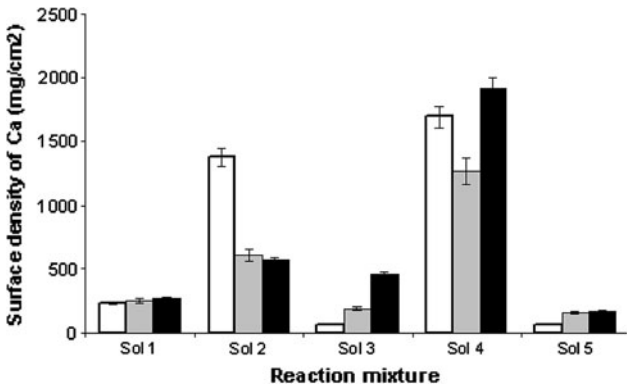

Fig. 3 Calcium encrustation from solution 1–5 at the end of the fifth week. *Open squares* without microorganisms, *grey squares* with *E. coli*, *filled squares* with *P. mirabilis*

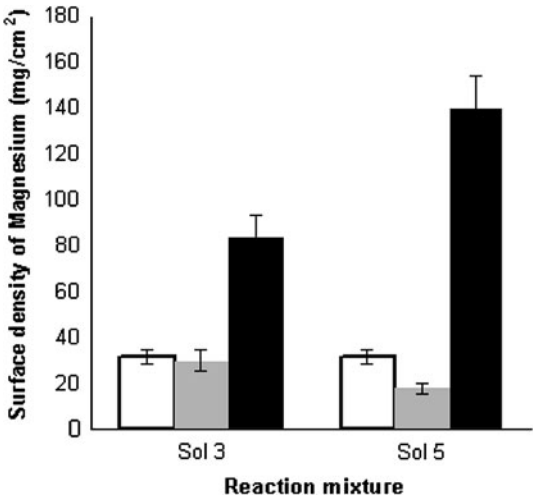

Fig. 4 Magnesium encrustation from solution 3 and solution 5 at the end of the fifth week. *Open squares* without microorganisms, *grey squares* with *E. coli*, *filled squares* with *P. mirabilis*

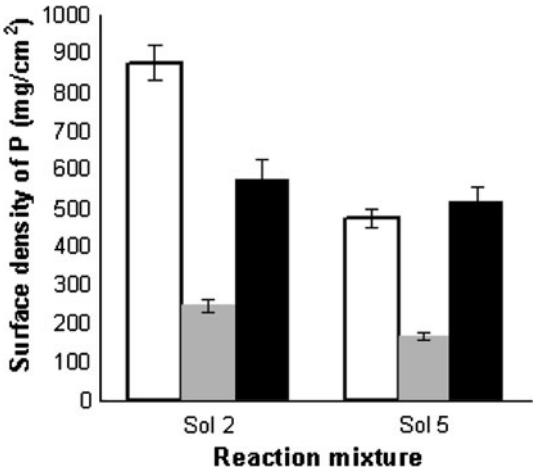

Fig. 5 Phosphorous encrustation from solution 2 and solution 5 at the end of the fifth week. *Open squares* without microorganisms, *grey squares* with *E. coli*, *filled squares* with *P. mirabilis*

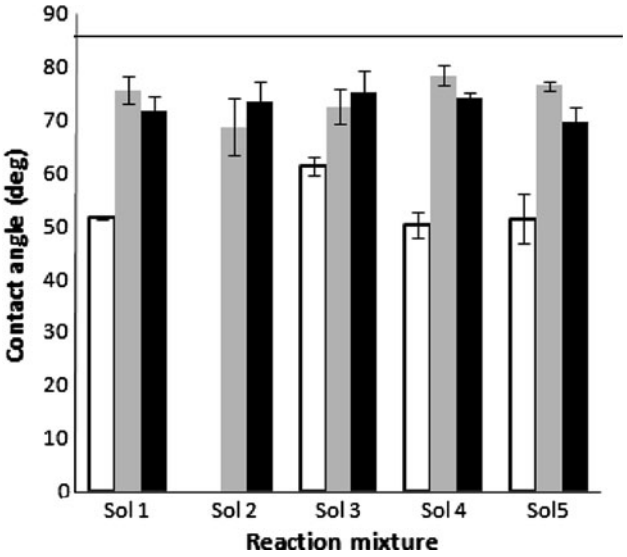

Fig. 6 Changes in hydrophobicity upon encrustaion in the fifth week. (—) contact angle of virgin PU (87.6°) (sol 2 without organisms could not be measured). *Open squares* without microorganisms, *grey squares* with *E. coli*, *filled squares* with *P. mirabilis*

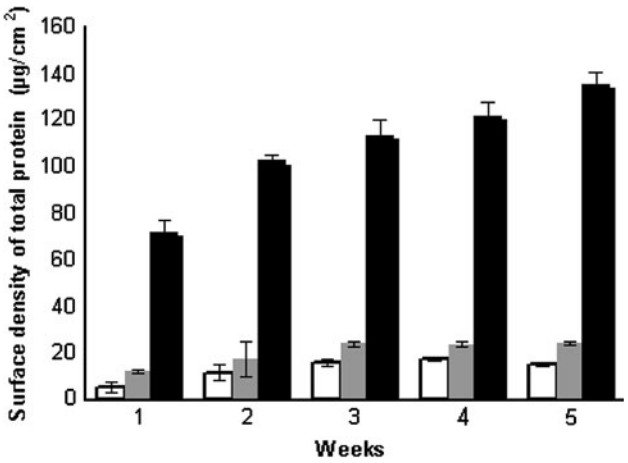

Fig. 7 Surface density of total protein adhered in the presence of *E. coli* and *P. mirabilis*. *Open squares* BSA, *grey squares* BSA + *E. coli*, *filled squares* BSA + *P. mirabilis*

At the end of fifth week pH of the solutions with *P. mirabilis* increased from an initial value of 6 to 12–13 (Fig. 9) and the highest pH range was with solution 5. The number of bacterial cells adhered per square centimeter of PU was higher in protein solution ($\sim 10^{12}$–10^{16}) than the salt solutions which was in the range of 10^{2}–10^{5} (Fig. 10).

Microscopic irregularities on the surface of the film before and after encrustation were observed with AFM (Fig. 11). The surface roughness increased on encrustation from 12 nm (virgin film) to 140 nm (sol: 1 + *E. coli*) and 330 nm (sol: 1 + *P. mirabilis*). The average roughness of the film treated with solution 1 are tabulated in Table 2.

FTIR spectra of all the samples were analyzed in the range of 1,700–1,750 cm^{-1} for the carbonyl group and 3,288–3,304 cm^{-1} 1 for the NH and OH groups. No significant changes were observed in the spectrum of samples analyzed, indicating the absence of any chemical reaction on the surface (Fig. 12).

Discussion

Urine is a complex milieu whose contents influence bacterial adhesion to the biomaterial. Encrustation of ureteral stents is due to the deposition of (1) organic layer (conditioning film) (2) uropathogens, and (3) salts in the urine.

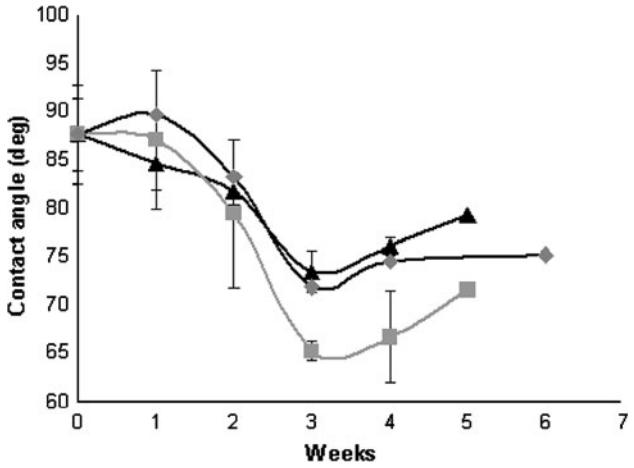

Fig. 8 Changes in the hydrophobicity upon BSA and bacterial adhesion. *Grey diamonds* BSA, *grey squares* BSA + *E. coli*, *filled triangles* BSA + *P. mirabilis*

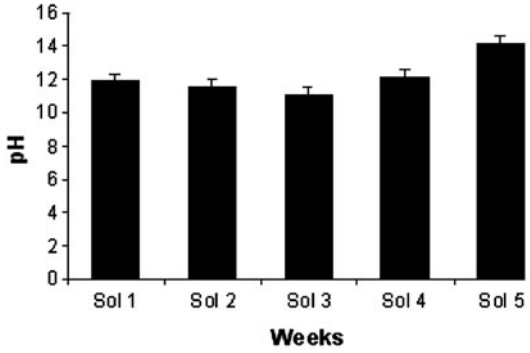

Fig. 9 Increase in pH with *P. mirabilis* in the fifth week

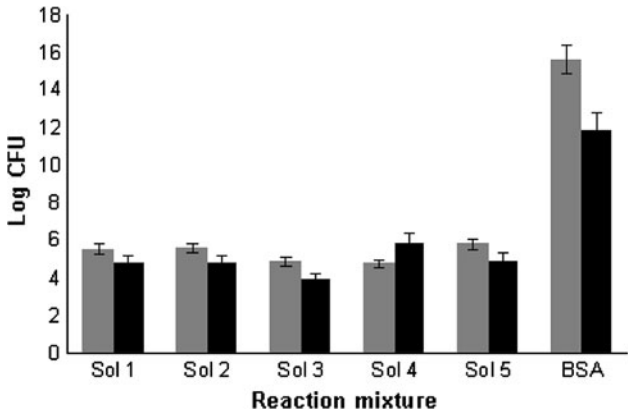

Fig. 10 Adherent bacteria in the fifth week. *Grey squares, E. Coli*; *filled squares, P. mirabilis*

Surface properties of the stent, including microscopic irregularities, hydrophobicity, and its charge affect the quantity as well as the type of deposition. Calcium oxalate is a common encrustant because of its poor solubility (0.2 mmol/L). The rate of encrustation is affected by the concentration of C_2O_4 as opposed to the amount of Ca^{2+} ions in the solution [21]. Salts used in this study are the basic salts of hydroxyl apatite [22] and struvite [23]. Artificial urine [19] is used to mimic the in vivo encrustation pattern on stents and the concentrations of individual salt solutions (sol 1–4) used are same as that of artificial urine.

The concentration of individual salts encrusted on the polyurethane film clearly demonstrates that the presence of sodium ions and ammonia enhances calcium encrustation, whereas magnesium ions depress calcium adhesion. Magnesium ion is well known for its anticalcification activity [24] and the current experiment also validates it. Both the organisms increase calcium encrustation in the presence of magnesium, whereas the rate of encrustation with other salts. The increased pattern of encrustation in the presence of *E. coli* in sol 1, sol 3, and sol 5 is due its biomineralization effect [25]. The negatively charged biomolecules inside and outside the bacterium interact with the Ca^{2+} ions to provide nucleation sites and act as a modifier to induce nucleation, growth, and aggregation of COM crystals. The CaOx crystal transforms itself to a stable crystalline form calcium oxalate monohydrate (COM) from the calcium oxalate dihydrate (COD) form.

Increased encrustation with magnesium and *E. coli* is attributed to the stabilization effect of this ion on *E. coli* [26], which leads to its decreased anti-calcification activity. Formation of struvite stones containing Mg^{2+} ions is due to the fact that these ions are also governed thermodynamically by their solubility product; exceeding the solubility product on increased pH range results in the formation of ion clouds and precipitation of crystals [2]. In the case of sol 2 the amount of calcium encrusted is higher due to the salting out effect of the sodium ions present in this solution [27], whereas effect of these sodium ions are reduced in the presence of *E. coli* because these ions regulate the acid resistance genes namely *gadE*, *gadA,* and *gadBC* which helps the organisms to survive even at the lowest pH (2) [28]. The amount of calcium encrusted in the case of sol 4 with *E. coli* is less when compared to that of *P. mirabilis* and without any organism. This could be due to the fact that ammonia is an essential growth factor for *E. coli* and is transported by the organism's ammonia transport channel AmtB [29], thereby decreasing its amount. With *P. mirabilis,* except for sol 2, irrespective of the type of salt, encrustation of calcium was higher. This could be due to the fact that these swarming cells exhibit high urease activity [30] which was also seen in the form of increased pH (Fig. 7). An increased encrustation of calcium was found in sol 4 and sol 5 with *P. mirabilis* than in the presence of *E. coli*, which is attributed to the increased urease activity induced by citrate ions in the artificial urine (sol 5) [31] and high concentration of ammonia in case of sol 4, which turns the solution more alkaline. In the case of sol 2, sodium ion acts

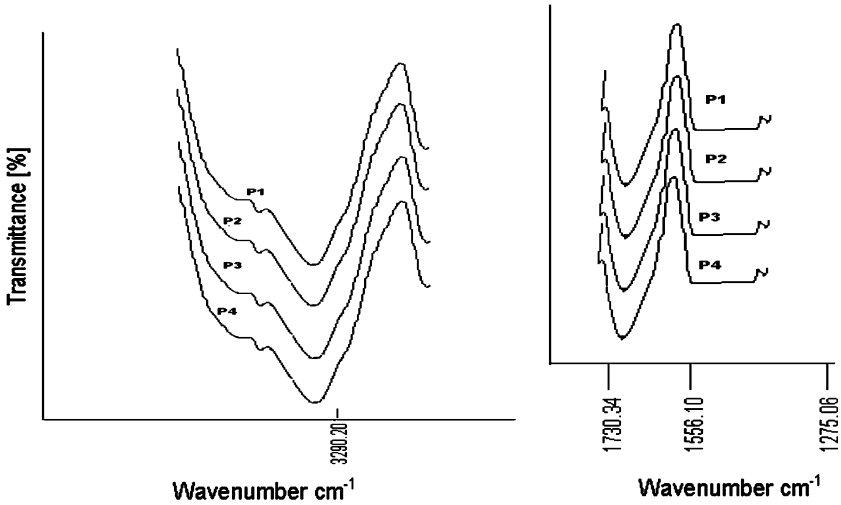

Fig. 11 **a** FTIR spectra of NH region located between 3,288 and 3,304 cm^{-1} bands **b** FTIR spectra of C==O region located between 1,700 and 1,750 cm^{-1} P1-Virgin PU film, P2-sol 4 treated, P3-sol 4 + *E. coli* treated, P4-sol 4 + *P. mirabilis* treated

Table 2 Roughness of the films after encrustation (5th week solution 1 treated sample)

	Mean roughness (nm)
Virgin film	12
Solution 1 + *E. coli*	140
Solution 1 + *P. mirabilis*	330

as an inhibitor of the enzyme urease [32] as a result of which the salting out effect of sodium as well as the urease activity is reduced. This leads to less encrustation when compared with the control (without organisms) and with *E. coli*. There exists a negative correlation between the amount of calcium encrusted as a function of time and the hydrophobicity of the corresponding polyurethane surface (for sol 1 = −0.98, sol 3 = −0.65, sol 4 = −0.96, sol 5: −0.97) in the absence of micro organisms. This indicates that as salts deposit the surface turns more hydrophilic. Hydrophilic *E. coli* (determined by water contact angle) adheres to the film, so a decrease in the hydrophobicity of the polymer surface could be attributed to the number of bacterial cells adhered (CFU) [33], but there exists a poor correlation between the CFU adhered and the change in hydrophobicity of the surface, which could be due to the fact that encrusted salts affect the polymer surface properties. Nanoscale roughness facilitates encrustation in two ways: (1) by providing more active sites for greater reactivity, and (2) by facilitating stronger adhesion of particles to the surface [34]. It is also clear from the current study, that the roughness of the film increases after encrustation which demonstrates that encrustation leads to rough surfaces. It is well documented that rough surfaces favor attachment of microorganisms. The FTIR spectrum revealed no significant chemical shift after encrustation, indicating that no chemical bonds have been formed between the salts and the base polymer.

The second part of the study deals with the analysis of simultaneous adhesion of bacteria and bovine serum albumin on PU. Deposition of a conditioning film on the surface of a material is an important event which takes place immediately after implantation. The characteristic of this conditioning film plays a crucial role in the later attachment of the microorganisms [35]. There are two main factors which are to be considered while analyzing the surface modification due to encrustation and bacterial colonization, namely (1) the actual nature of the polymer films and (2) the effect of this polymer on the deposition and composition of the conditioning film. These in turn affect bacterial colonization [36].

It is hypothesized that binding of most abundant proteins, namely human serum albumin, tamm horsfal protein, and α1-micro globulin [37] found in urine form a defense against infection by binding to these organisms and flushing them out of the urinary tract. But in the current study, it is seen that surface density of protein increases with time and also more in the presence of microorganisms. The attachment in the presence of *P. mirabilis* is higher than in the presence of *E. coli*. There are studies which report that higher levels of calcium in urine increases bacterial adhesion to the uroepithelial cells, but their effect on stent is not clear [38]. Metabolic disorders such as hypercalciuria, hypocitraturia, hyperuricosuria, or hyperoxaluria accelerates encrustation of implants in a sterile environment [39]. Though encrustations in case of stone formers are higher when compared to the normal conditions, it could be due to the fact that excess of calcium ions could mediate adhesion of microorganisms and encrustation [34]. Although physico-chemical explanations to elucidate the mechanism of encrustation or infection-inhibiting materials are not available, some antibacterial agents serve as a binding for salts and induce encrustation. Certain antibacterial agents like heparin, phosphoryl cholin encompass both the properties, they inhibit bacterial adhesion with strong

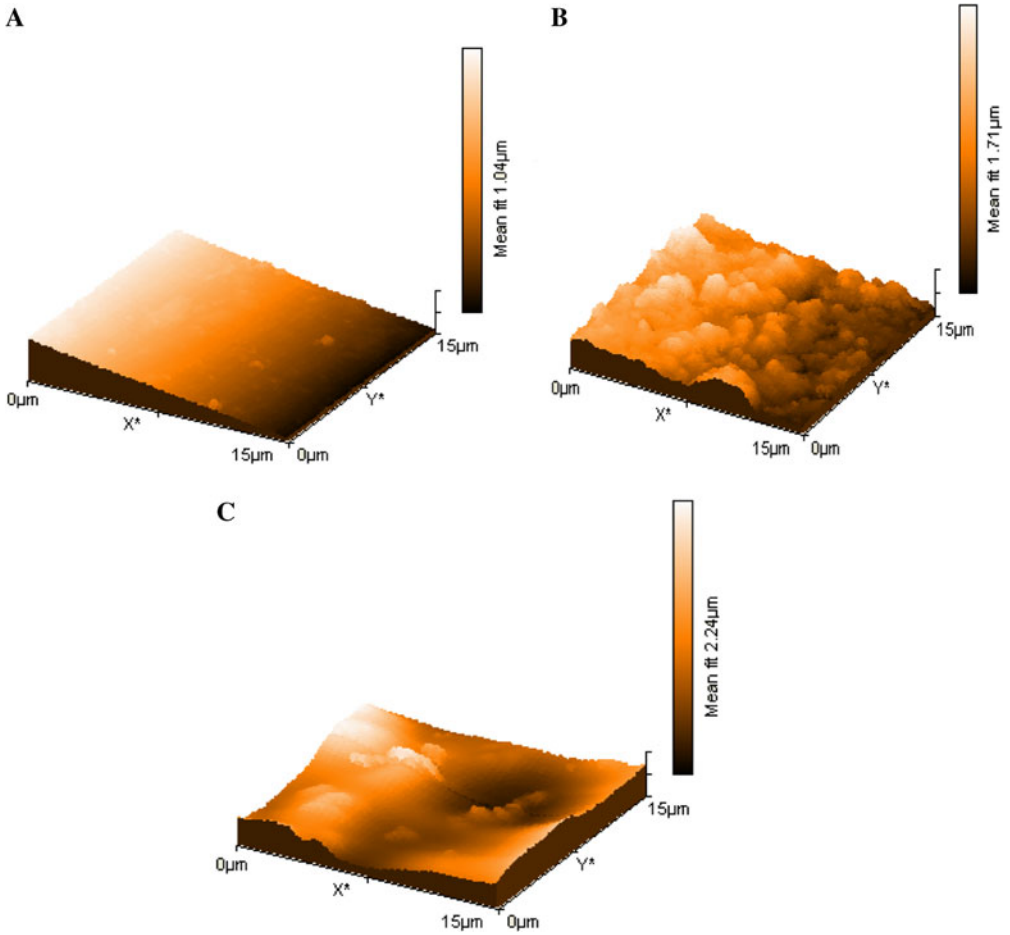

Fig. 12 AFM Image of (**a**) Virgin film (**b**) Encrusted fifth week film incubated with sol 1 + *E. coli* (**c**) sol 1 + *P. mirabilis*

electronegativity, with a considerable decrease in encrustation also [40]. As encrustation and biofilm formation are patho-biochemically associated, an ideal material is yet to be explored, but polyurethane and coated polyurethane materials find wide applications as they give satisfactory results in short period [10]. The current findings also indicate that surface properties of the polymer are significantly affected by the surrounding body fluid.

Conclusion

In the sterile urine solution, magnesium ions depress the encrustation of calcium, whereas sodium ions and ammonia enhance it. In the case of bacterial urine, encrustation of calcium was enhanced by magnesium. Calcium precipitation was higher in the presence of ammonia, urea, and urease. Hydrophobicity of the polymer surface decreases with encrustation, whereas protein adhesion turns the surface hydrophilic initially and later hydrophobic which needs rationalization. The interaction between the biomaterial and the individual urinary component must be well established to devise an ideal surface that resists bacterial adhesion and encrustation. The above-described methodology is a quick, efficient, and easy method that can be used to validate any new biomaterial under in vitro conditions before testing it on animal models and human trials.

Acknowledgment The authors thank Sophisticated Analytical Instrument Facility, IIT Madras, for the analytical support.

References

1. Jones DS, Bonner MC, Akay M, Keane PF, Gorman SP (1997) Sequential polyurethane-poly (methylmethacrylate) interpenetrating polymer networks as ureteral biomaterials: mechanical properties and comparative resistance to urinary encrustation. J Mater Sci Mater Med 8:713–717
2. Schierholz JM, Yücel N, Rump AFE, Beuth J, Pulverer G (2002) Antiinfective and encrustation-inhibiting materials—myth and facts. Int J Antimicrob Ag 19(6):511–516
3. Tunney MM, Gorman SP, Patrick S (1996) Medical device-related Infection. Rev Med Microbiol 7(4):195–210
4. Ben-Meir D, Golan S, Ehrlich Y, Livne PM (2009) Characteristics and clinical significance of bacterial colonization of ureteral double-J stents in children. J Pediatr Urol 5(5):355–358

5. Elves AWS, Feneley RCL (1997) Long-term urethral catheterization and the urine-biomaterial interface. Br J Urol 80:1–5
6. Costerton JW, Cheng KJ, Geesey GG, Ladd TI, Nickel JC, Dasgupta M, Marrie TJ (1987) Bacterial biofilms in nature and disease. Ann Rev Microbiol 41:435–464
7. Santin M, Motta A, De Nyer SP, Cannas M (1999) Effect of the urine conditioning film on ureteral stent encrustation and characterization of its protein composition. Biomaterials 20:1245–1251
8. Zhong P, Chuong CJ, Goolsby RD, Preminger GM (1992) Microhardness measurements of renal calculi: regional differences and effects of microstructure. J Biomed Mater Res 26:1117–1130
9. Gorman SP, Jones DS, Bonner MC, Akay M, Keane PF (1997) Mechanical performance of polyurethane ureteral stents in vitro and ex vivo. Biomaterials 18:1379–1383
10. Nandakumar V, Sunil S, Karthik J, Mukesh D (2010) Polymers as ureteral stents. J Endourol 24(2):191–198
11. Clapham L, Mclean RJC, Nickel JC, Downey J, Costerton JW (1990) The influence of bacteria on struvite crystal habit and its importance in urinary stone formation. J Cryst Growth 104:475–484
12. Jones DS, Djokic J, Gorman SP (2005) The resistance of polyvinylpyrrolidone–Iodine–poly(-caprolactone) blends to adherence of *Escherichia coli*. Biomaterials 26(14):2013–2020
13. Stickler DJ, Morris NS, Winters C (1999) Simple physical model to study formation and physiology of biofilms on urethral catheters. Methods Enzymol 310:494–501
14. Melcher LR, Masouredis SP, Reed R (1953) The immunological relationship between human and bovine serum albumin. J Immunol 70:125–128
15. Multanen M, Talja M, Hallanvuo S, Siitonen A, Vaèlima T, Tammela TLJ, Seppaèlaè J, Toèrmaèlaè P (2000) Bacterial adherence to ofloxacine-blended polylactonecoated self-reinforced L-lactic acid polymer urological stents. British J Urol Int 86:966–969
16. Jones DS, Garvin CP, Dowling D, Donnelly K, Gorman SP (2006) Examination of surface properties and in vitro biological performance of amorphous diamond-like carbon-coated polyurethane. J Biomed Mater Res B Appl Biomater 78B(2):230–236
17. Grases F, Söhnel O, Costa-Bauzá A, Ramis M, Wang Z (2001) Study on concretions developed around urinary catheters and mechanisms of renal calculi development. Nephron 88:320–328
18. Cormio L, La Forgia P, La Forgia D, Siitonen A, Ruutu M (1997) Is it possible to prevent bacterial adhesion onto ureteric stents? Urol Res 25:213–216
19. Petas A, Varkila JV, Siitonen A, Valimaa T, Talja M, Taari K (1998) Bacterial adherence to the self-reinforced polyglycolic acid and self-reinforced polylactic acid 96 urological spiral stents in vitro. Biomaterials 19:677–681
20. Clarke S, Davies MC, Roberts CJ, Tendler SJB, Williams PM, Lewis AL (2001) Atomic force microscope and surface plasmon resonance investigation of polymer blends of poly ([2-(methacryloyloxy)ethyl]phosphorylcholineco-lauryl methacrylate) and poly (lauryl methacrylate). Macromolecules 34(12):4166–4172
21. El-Shall H, Jeon JH, Abdel-Aal EA, Khan S, Gower L, Rabinovich Y (2004) A study of primary nucleation of calcium oxalate monohydrate: II Effect of urinary species. Cryst Res Technol 39:222–229
22. Parhi P, Ramanan A, Ray AR (2004) A convenient route for the synthesis of hydroxyapatite through a novel microwave-mediated metathesis reaction. Mater Lett 58(27–28):3610–3612
23. Harada H, Shimizu Y, Miyagoshi Y, Matsui S, Matsuda T, Nagasaka T (2006) Predicting struvite formation for phosphorus recovery from human urine using an equilibrium model. Water Sci Technol 54:247–255
24. Feagin FF, Walker AA, Pigman W (1969) Evaluation of the calcifying characteristics of biological fluids and inhibitors of calcification. Calcif Tissue Int 4(1):231–244
25. Chen L, Shen Y, Jia R, Xie A, Huang B, Cheng X, Zhang Q, Guo R (2007) The role of Escherichia coliform in the biomineralization of calcium oxalate crystals. Eur J Inorg Chem 20:3201–3207
26. Abelson PH, Aldous E (1950) Ion antagonisms in microorganisms: interference of normal magnesium metabolism by nickel, cobalt, cadmium, zinc, and manganese. J Bacteriol 60:401–413
27. Hey MJ, Jackson DP, Yan H (2005) The salting-out effect and phase separation in aqueous solutions of electrolytes and poly (ethylene glycol). Polymer 46:2567–2572
28. Richard H, Foster JW (2007) Sodium regulates *Escherichia coli* acid resistance, and influences GadX- and GadW-dependent activation of gadE. Microbiology 153:3154–3161
29. Nygaard TP, Rovira C, Peters GH, Jensen M (2006) Ammonium recruitment and ammonia transport by *E. coli* ammonia channel AmtB. Biophys J 91:4401–4412
30. Liedl Bernhard (2001) Catheter-associated urinary tract infections. Curr Opin Urol 11(1):75–79
31. Hedelin H, Grenabo L, Hugosson J, Pettersson S (1989) The influence of zinc and citrate on urease-induced urine crystallisation. Urol Res 17(3):177–180
32. Fasman GD, Niemann C (1951) A reinvestigation of the kinetics of the urease-catalyzed hydrolysis of urea. I. The activity of urease in the presence of sodium and potassium phosphate. J Am Chem Soc 73(4):1646–1650
33. Reid G, Lam D, Policova Z, Neumann AW (1993) Adhesion of two uropathogens to silicone and lubricious catheters: Influence of pH, urea and creatinine. J Mater Sci Mater Med 4:17–22
34. Egan TJ, Rodgers AL, Siele T (2004) Nucleation of calcium oxalate crystals on an imprinted polymer surface from pure aqueous solution and urine. J Biol Inorg Chem 9:195–202
35. Pavithra D, Doble M (2008) Biofilm formation, bacterial adhesion and host response on polymeric implants? Issues and prevention. J Biomed Mater 3:034003
36. Reid G, Busscher HJ, Sharma S, Mittelman MW, McIntyre S (1995) Surface properties of catheters, stents and bacteria associated with urinary tract infections. Surf Sci Rep 21:251–273
37. Orskov I, Ferencz A, Orskov F (1980) Tamm Horsfall protein or uromucoid is the normal urinary slime that traps type 1 fimbriated *Escherichia coli*. Lancet 1:887
38. Apicella LL, Sobota AE (1990) Increased risk of urinary tract infection associated with the use of calcium supplements. Urol Res 18:213–217
39. Multanen M, Tammela TLJ, Laurila M, Seppala J, Valimaa T, Tormala P, Talja M (2002) Biocompatibility, encrustation and biodegradation of ofloxacine and silver nitrate coated poly-L-lactic acid stents in rabbit urethra. Urol Res 30:227–232
40. Riedl CR, Witkowski M, Plas E, Pflueger H (2002) Heparin coating reduces encrustation of ureteral stents: a preliminary report. Int J Antimicrob Agents 19(6):507–510